HHS Public Access
Author manuscript
Clin Radiol. Author manuscript; available in PMC 2015 December 09.

Published in final edited form as:
Clin Radiol. 2014 October ; 69(10): e398–e403. doi:10.1016/j.crad.2014.06.012.

Assessment of Change in Prostate Volume and Shape Following Surgical Resection Through Co-Registration of *In Vivo* MRI and Fresh Specimen *Ex Vivo* MRI

Clement Orczyk, MD MSc[1,3,4,5,6,7], **Samir S Taneja, MD**[1,2], **Henry Rusinek, PhD**[1,2], and **Andrew B Rosenkrantz, MD**[2]

[1]Division of Urologic Oncology, Department of Urology, New York University Langone Medical Center, New York, NY

[2]Department of Radiology, New York University Langone Medical Center, New York, NY

[3]Department of Urology, Côte de Nacre University Hospital, Caen, France

[4]CNRS, UMR 6301 ISTCT, CERVOxy. GIP CYCERON, F-14074 Caen, France

[5]CEA, DSV/I2BM, UMR 6301 ISTCT, F-14074 Caen, France

[6]UNICAEN, UMR 6301 ISTCT, F-14074 Caen, France

[7]Normandie Univ, France

Abstract

Correspondence: Dr Clement Orczyk, Department Of Urology, Côte de Nacre University Hospital, Caen, France, **UMR ISTCT 6301** - CNRS, CEA, Université de Caen Basse-Normandie, "Imaging and Therapeutical Strategies in Cerebral and Tumoral pathologies", CERVOxy team "Hypoxia, cerebrovascular and tumoral pathophysiologies", CYCERON, Bd Henri Becquerel, BP5229, F-14074 CAEN cedex France, Phone: +33 6 22 48 26 44, Fax: +33 2 31 06 49 47, clementorczyk@yahoo.fr.
All authors: NYU Langone Medical Center, 550 First Avenue, New York, NY 10016

Disclosure and financial interest:
Clement Orczyk, Henry Rusinek and Andrew B Rosenkrantz have nothing to disclose.
Samir S Taneja is consultant for Eigen, consultant and scientific investigator for GTX, scientific investigator for Steba Biotech, speaker for Janssen, has royalties from Elsevier. No direct financial conflict of interest is identified.

Author's Contributions:
Clement Orczyk MD MSc, Samir S Taneja MD, Henry Rusinek PhD, Andrew B Rosenkrantz MD

1. guarantor of integrity of the entire study *C ORCZYK*
2. study concepts and design- *C ORCZYK, SS TANEJA, H RUSINEK, AB ROSENKRANTZ*
3. literature research *C ORCZYK, AB ROSENKRANTZ, H RUSINEK, SS TANEJA*
4. clinical studies *SS TANEJA, AB ROSENKRANTZ*
5. experimental studies / data analysis *C ORCZYK, H RUSINEK, AB ROSENKRANTZ*
6. statistical analysis *C ORCZYK*
7. manuscript preparation *C ORCZYK, AB ROSENKRANTZ*
8. manuscript editing. C ORCZYK, *SS TANEJA, H RUSINEK, AB ROSENKRANTZ.*

AIM—To compare the size and shape of the prostate between *in-vivo* and fresh *ex-vivo* magnetic resonance imaging (MRI), in order to quantify alterations in the prostate resulting from surgical resection.

MATERIAL AND METHOD—Ten patients who had undergone 3 T prostate MRI using a phased-array coil and who were scheduled for prostatectomy were included in this prospective study. The *ex-vivo* specimen underwent MRI prior to formalin fixation or any other histopathological processing. Prostate volume *in vivo* and *ex vivo* was assessed using planimetry. Prostate shape was assessed by calculating ratios between the diameters of the prostate in all three dimensions.

RESULTS—Mean prostate volume was significantly smaller *ex vivo* than *in vivo* (39.7±18.6 versus 50.8±26.8 cm^3; p=0.008), with an average change in volume of −19.5%. The right-to-left (RL)/anteroposterior (AP) ratio of the prostate, representing the shape of the prostate within its axial plane, was significantly larger *ex vivo* than *in vivo* (1.33±0.14 versus 1.21±0.12; p=0.015), with an average percent change in RL/AP ratio of the prostate of +12.2%. There was no significant difference between *in-vivo* and *ex-vivo* acquisitions in terms of craniocaudal (CC)/AP (p=0.963, median change=−2.1%) or RL/CC (p=0.265, median change=+1.3%) ratios.

CONCLUSION—The observed volume and shape change following resection has not previously been assessed by comparison of *in-vivo* and fresh *ex-vivo* MRI and likely represents loss of vascularity and of connective tissue attachments in the *ex-vivo* state. These findings have implications for co-registration platforms under development to facilitate improved understanding of the accuracy of MRI in spatial localization of prostate tumours.

INTRODUCTION

Multiparametric magnetic resonance imaging (MRI) (mpMRI) of the prostate is increasingly being used for a broad array of clinical applications, including tumour detection and localization[12], planning of targeted biopsies[3], treatment selection[4], preoperative planning[4], and monitoring of active surveillance[5]. These applications rely upon accurate spatial localization of tumour on mpMRI. An understanding of the accuracy of such localization is important for proper incorporation of imaging findings on mpMRI into clinical practice. Such validation has been attempted in a large volume of previous studies via attempted correlation of *in-vivo* MRI images with histopathological findings observed following radical prostatectomy[6]. However, past studies have generally not considered or accounted for the potential impact of the surgical procedure itself upon the size and shape of the prostate. It is possible that alterations in prostate vascularity and elasticity resulting simply from the prostatectomy may significantly change prostate morphology[7], thereby impairing the ability to reliably assess the accuracy of tumour localization at *in-vivo* MRI via correlation with histopathological slides, and adjustments to correct for such changes would be warranted in future research. Thus, in the present study, the size and shape of the prostate between *in-vivo* and *ex-vivo* prostate MRI images were compared, in an effort to quantify changes resulting from surgical resection. The *ex-vivo* prostate was imaged fresh, prior to formalin fixation or any other processing.

MATERIALS AND METHODS

Patients

This prospective study was HIPAA-compliant and approved by the institutional review board. All patients signed written informed consent prior to participation. Ten patients (mean age 65±5.94 years) with biopsy-proven prostate cancer scheduled to undergo radical prostatectomy were included. Mean preoperative prostate-specific antigen (PSA) level 6.17±0.43 ng/ml (median 6.2ng/ml). All patients had undergone a preoperative 3 T mpMRI of the prostate, which is routinely performed following a positive prostate biopsy at New York University Langone Medical Center. In addition, the fresh *ex-vivo* prostate specimen underwent MRI, as described below. No patient received therapy between MRI and surgery. Mean delay between MRI and surgery was 45.4±54 days (median 33 days). Final histopathological stages were: pT2c (*n*=3), pT3a (*n*=6), and pT3b (*n*=1). Final Gleason scores were 6 (3+3) in one case, 7 (3+4) in five cases, 7 (4+3) in four cases.

In-vivo MRI acquisition

Patients underwent preoperative MRI of the prostate using a 3 T system (Magnetom Trio, Siemens Healthcare, Erlangen, Germany) using a pelvic phased-array coil. The protocol included an axial turbo-spin echo (TSE) T2-weighted imaging (T2WI) sequence of the prostate and seminal vesicle [3600 ms repetition time (TR)/123 ms echo time (TE); 3 mm section thickness; 160 × 160 mm field of view (FOV); 256 × 256 matrix; parallel imaging factor of 2; three signals averaged]. Dynamic contrast-enhanced (DCE) imaging and diffusion-weighted imaging (DWI) were also performed, but not assessed as part of this study.

Surgical resection and *ex-vivo* MRI

All 10 patients underwent robotic-assisted radical prostatectomy, performed by a single surgeon with 15 years of experience (SST). The fresh surgical specimen was prepared by sewing a segment of urethral catheter into the prostatic urethra for preservation of urethral elongation. Within 12 h of resection and prior to formalin fixation, sectioning, or any other histopathological processing, the fresh specimen underwent *ex-vivo* MRI using the same 3 T system as for *in-vivo* imaging and comprising T2WI with sequence parameters matching *in-vivo* MRI aside from use of a rectangular FOV of 40% given the lack of surrounding pelvic tissues. During this delay, the specimen was maintained at 4°C to minimi ze tissue changes.

Assessment of prostate volume and shape—Analysis of the images was performed by a research fellow (C.O.), under supervision of a fellowship-trained abdominal radiologist (A.B.R.), with 5 years of experience in prostate MRI interpretation. The image analysis was performed using locally-developed in-house software (Firevoxel), which has previously been used to assess volume of other tissues [8].

Volume measurements of the *in-vivo* and *ex-vivo* prostate was achieved via planimetry, which has been previously shown to be an accurate method for this purpose [9]. First, the prostate was manually delineated on *in-vivo* and *ex-*vivo T2WI, excluding of surrounding peri-prostatic fat, the neurovascular bundles (if present *ex vivo*), the bladder neck, and the seminal vesicles. Subsequently, volume was computed on a voxel basis.

The shape of the prostate was assessed by initially measuring the largest diameter of the prostate in the anteroposterior (AP), right-to-left (RL), and craniocaudal (CC) dimensions. Then, the AP/RL, AP/CC, and RL/CC ratios were calculated *in vivo* and *ex vivo*.

Statistical assessment

Paired *t*-tests were used to compare prostate volume, the three linear dimensions of the prostate, and the three ratios between these linear dimensions representing prostate shape, between *in-vivo* and *ex-vivo* images for each case. The mean, standard deviation, and median percent changes in volume and in terms of the three ratios were computed between the *in-vivo* and *ex-vivo* images. All *p*-values are two-sided and considered statistically significant at $p<0.05$. Statistical analysis was performed using software (R, version 2.14.0, CRAN, Vienna, Austria) and Excel (version 2011, Microsoft, Redmond, WA, USA).

RESULTS

In-vivo and *ex-vivo* MRI acquisitions, as well as the described volume and shape measurements, were successfully performed in all 10 patients. The obtained volume and shape measurements are summarized in Table 1. Mean prostate volume was significantly smaller *ex vivo* than *in vivo* (39.7±18.6 versus 50.8±26.8 cm^3, respectively; $p=0.008$), with an average percent change in size of the prostate of −19.5%, equivalent to a 23% greater volume of the prostate on *in-vivo*, compared with *ex-vivo*, MRI (Figure 1). In addition, there was a decrease in size of the prostate in all three dimensions between *ex-vivo* and *in-vivo* scans: RL dimension, 4.82±0.77 cm versus 5.05±0.92 cm, $p=0.015$; AP dimension, 3.62±0.56 cm versus 4.01±0.78 cm, $p=0.002$; CC dimension, 3.9±0.82 cm versus 4.09±1.40 cm, $p=0.087$.

The ratios between the three linear dimensions of the prostate were compared to assess for a tendency for the shape of the prostate to change between *in-vivo* and *ex-vivo* scans in a particular orientation (Fig. 2). The RL/AP ratio of the prostate, thus representing the shape of the prostate within its axial plane, was significantly larger *ex vivo* than *in vivo* (1.33±0.14 versus 1.21±0.12, respectively; $p=0.015$), with an average percent change in RL/AP ratio of the prostate of +11.3%. There was no significant difference between scans in terms of CC/AP ratio ($p=0.963$, average percent change=−2.1%) or RL/CC ratio ($p=0.265$, average percent change = +1.3%). Images from a representative case are shown in Fig. 3.

DISCUSSION

In the present study, a significant difference was observed in volume of the prostate following surgical resection, with an average loss of 19.5% of the gland's volume. To the authors' knowledge, this finding has not been previously assessed by comparison of *in-vivo* and *ex-vivo* prostate MRI. The use of MRI for this purpose facilitated the determination of prostate dimensions and volume. Furthermore, via careful evaluation of *ex-vivo* T2WI, it was possible to include within the *ex-vivo* volume measurement only the prostate gland itself, while excluding all surrounding tissues. This is important because the resected prostate is intimately associated with surrounding tissue such as fat, pelvic fascia, or the neurovascular bundles, depending of the operative technique. These adjacent structures can confound accurate specimen measurements of the specimen, but cannot be removed physically; doing so may negatively impact evaluation of the surgical margin status [10] and lead to improper staging. Thus, the present approach to evaluating the *ex-vivo* prostate via MRI allowed for accurate measurements after image-based exclusion of peri-prostatic structures, while preserving the integrity of the specimen for further histopathological evaluation.

An additional key aspect of the present method was that the *in-vivo* MRI was performed without use of an endorectal coil, which potentially could compress and deform the prostate, thereby confounding the comparison with the *ex-vivo* prostate. For instance, Heijmink *et al*.[11] reported an approximately 18% difference in volume of the prostate evaluated by MRI between examinations performed with and without an endorectal coil. Thus, in the present study, the only difference between the two acquisitions was the interval surgical procedure itself.

This finding in terms of volume reduction is important given the role of correlative studies between multiparametric and histology, which have often used radical prostatectomy specimens as the reference standard, in influencing the clinical integration of mpMRI [1213]. Numerous past studies have accounted for shrinkage of the prostate attributed to the process of histopathological processing [14–16]. This step accounts for change in volume due to tissue dehydration that results from formalin fixation and paraffin embedding, but does not correct for the loss of volume due to the surgery procedure, as per the current report. It is possible that a greater degree of volume correction may be needed than in past studies given the additional observed contribution of the surgical procedure to volume changes.

Although the decrease in volume of the *ex-vivo* prostate was due to a reduction in size in all dimensions, this size reduction was not homogeneous between the three dimensions, as indicated by the significant difference in the AP/RL ratio between the two acquisitions. Thus, the surgical procedure is associated with a change in the shape of the prostate in the axial plane. This spatial deformation may relate to a loss of connective tissue attachments, for instance to the dorsal venous complex or lateral pelvic fascia[17], that maintain the shape of the *in-vivo* prostate, thereby releasing the prostate in the *ex-vivo* state and resulting in a change in shape given the prostate's viscoelastic properties[18]. Therefore, magnification alone of histopathological images, in order to account for the volume reduction, is not likely to be sufficient to achieve optimal co-registration of *in-vivo* prostate MRI and histopathological images; rather, as correlation of lesions is predominantly performed within the axial plane, measures are needed to correct for the deformation within this plane resulting from the surgery.

Numerous reports describe co-registration platforms currently in development from a variety of centres [192021]. The present findings support the need for such platforms to employ a three-dimensional deformable approach in order to achieve optimal correlation. The resulting improved compensation for changes in volume and shape will be of much value when performing co-localization of small tumours between MRI and histology.

Limitations of the present study include the small sample size, lack of assessment of reproducibility of the volume metrics, and lack of confirmation of suggested reasons for the change in prostate volume following prostatectomy.

In conclusion, via performance of MRI of fresh *ex-vivo* prostatectomy specimens, a significant decrease of approximately 19% was demonstrated in the volume of the prostate resulting from this surgical procedure. In addition, the surgery resulted in a significant change in shape of the prostate in the axial plane. It is, therefore, advised that co-registration platforms employ three-dimensional deformable transformation to compensate for this volume loss and change in orientation in the axial plane, in order to achieve reasonable accuracy in correlation. More accurate co-registration incorporating the present findings will facilitate improved understanding of the accuracy of mpMRI in the spatial localization of tumours within the prostate.

ACKNOWLEDGEMENTS

The authors acknowledge The Joseph and Diane Steinberg Charitable Trust and the Grant 1UL1RR029893 from the National Center for Research Resources, National Institutes of Health for support. C.O., H.R. and A.B.R. have nothing to disclose. S.S.T. is consultant for Eigen, consultant and scientific investigator for GTX, scientific investigator for Steba Biotech, speaker for Janssen, has royalties from Elsevier.

REFERENCES

1. Dickinson L, Ahmed HU, Allen C, et al. Magnetic resonance imaging for the detection, localisation, and characterisation of prostate cancer: recommendations from a European consensus meeting. Eur Urol. 2011; 59:477–494. [PubMed: 21195536]
2. Rosenkrantz AB, Deng F-M, Kim S, et al. Prostate cancer: multiparametric MRI for index lesion localization—a multiple-reader study. AJR Am J Roentgenol. 2012; 199:830–837. [PubMed: 22997375]
3. Rosenkrantz AB, Taneja SS. Targeted prostate biopsy: opportunities and challenges in the era of multiparametric prostate magnetic resonance imaging. J Urol. 2012; 188:1072–1073. [PubMed: 22901570]
4. Rosenkrantz AB, Scionti SM, Mendrinos S, Taneja SS. Role of MRI in minimally invasive focal ablative therapy for prostate cancer. AJR Am J Roentgenol. 2011; 197:W90–W96. [PubMed: 21701001]
5. Villers A, Lemaitre L, Haffner J, et al. Current status of MRI for the diagnosis, staging and prognosis of prostate cancer: implications for focal therapy and active surveillance. Curr Opin Urol. 2009; 19:274–282. [PubMed: 19325494]
6. Villers A, Puech P, Mouton D, Leroy X, Ballereau C, Lemaitre L. Dynamic contrast enhanced, pelvic phased array magnetic resonance imaging of localized prostate cancer for predicting tumor volume: correlation with radical prostatectomy findings. J Urol. 2006; 176:2432–2437. [PubMed: 17085122]
7. Terris MK, Stamey TA. Determination of prostate volume by transrectal ultrasound. J. Urol. 1991; 145:984–987. [PubMed: 2016815]
8. Ko JP, Berman EJ, Kaur M, et al. Pulmonary Nodules: growth rate assessment in patients by using serial CT and three-dimensional volumetry. Radiology. 2012; 262:662–671. [PubMed: 22156993]
9. Matthews GJ, Motta J, Fracchia J. The accuracy of transrectal ultrasound prostate volume estimation: clinical correlations. J Clin Ultrasound. 1996; 24:501–505. [PubMed: 8906481]

10. Berney DM, Wheeler TM, Grignon DJ, et al. International Society of Urological Pathology (ISUP) consensus conference on handling and staging of radical prostatectomy specimens. Working group 4: seminal vesicles and lymph nodes. Mod Pathol. 2011; 24:39–47. [PubMed: 20818343]
11. Heijmink SWTPJ, Scheenen TWJ, van Lin ENJT, et al. Changes in prostate shape and volume and their implications for radiotherapy after introduction of endorectal balloon as determined by MRI at 3T. Int J Radiat Oncol Biol Phys. 2009; 73:1446–1453. [PubMed: 19036532]
12. Turkbey B, Mani H, Aras O, et al. Correlation of magnetic resonance imaging tumor volume with histopathology. J. Urol. 2012; 188:1157–1163. [PubMed: 22901591]
13. Mazaheri Y, Hricak H, Fine SW, et al. Prostate tumor volume measurement with combined T2-weighted imaging and diffusion-weighted MR: correlation with pathologic tumor volume. Radiology. 2009; 252:449–457. [PubMed: 19703883]
14. Schned AR, Wheeler KJ, Hodorowski CA, et al. Tissue-shrinkage correction factor in the calculation of prostate cancer volume. Am J Surg Pathol. 1996; 20:1501–1506. [PubMed: 8944043]
15. Schmid HP, McNeal JE. An abbreviated standard procedure for accurate tumor volume estimation in prostate cancer. Am J Surg Pathol. 1992; 16:184–191. [PubMed: 1733351]
16. Jonmarker S, Valdman A, Lindberg A, Hellström M, Egevad L. Tissue shrinkage after fixation with formalin injection of prostatectomy specimens. Virchows Arch. 2006; 449:297–301. [PubMed: 16909262]
17. Lepor H. A review of surgical techniques for radical prostatectomy. Rev Urol. 2005; 7:S11–S17. [PubMed: 16985892]
18. Zhang M, Nigwekar P, Castaneda B, et al. Quantitative characterization of viscoelastic properties of human prostate correlated with histology. Ultrasound Med Biol. 2008; 34:1033–1042. [PubMed: 18258350]
19. Orczyk C, Rusinek H, Rosenkrantz AB, et al. Preliminary experience with a novel method of three-dimensional co-registration of prostate cancer digital histology and *in vivo* multiparametric MRI. Clin Radiol. 2013; 68:e652–e658. [PubMed: 23993149]
20. Ward AD, Crukley C, McKenzie CA, et al. Prostate: registration of digital histopathologic images to *in vivo* MR images acquired by using endorectal receive coil. Radiology. 2012; 263:856–864. [PubMed: 22474671]
21. Mazaheri Y, Bokacheva L, Kroon D-J, et al. Semi-automatic deformable registration of prostate MR images to pathological slices. J Magn Reson Imaging. 2010; 32:1149–1157. [PubMed: 21031521]

Highlights

- Preresection prostates to freshly resected prostates were compared for volume and shape.
- Volume and shape were quantified using in vivo and ex vivo T2w MRI at 3T.
- A −19.5% statistically significant volume decrease was reported after resection.
- Significant change in shape is observed on the axial slices.
- Findings impact MRI-histology correlation studies and further clinical deductions.

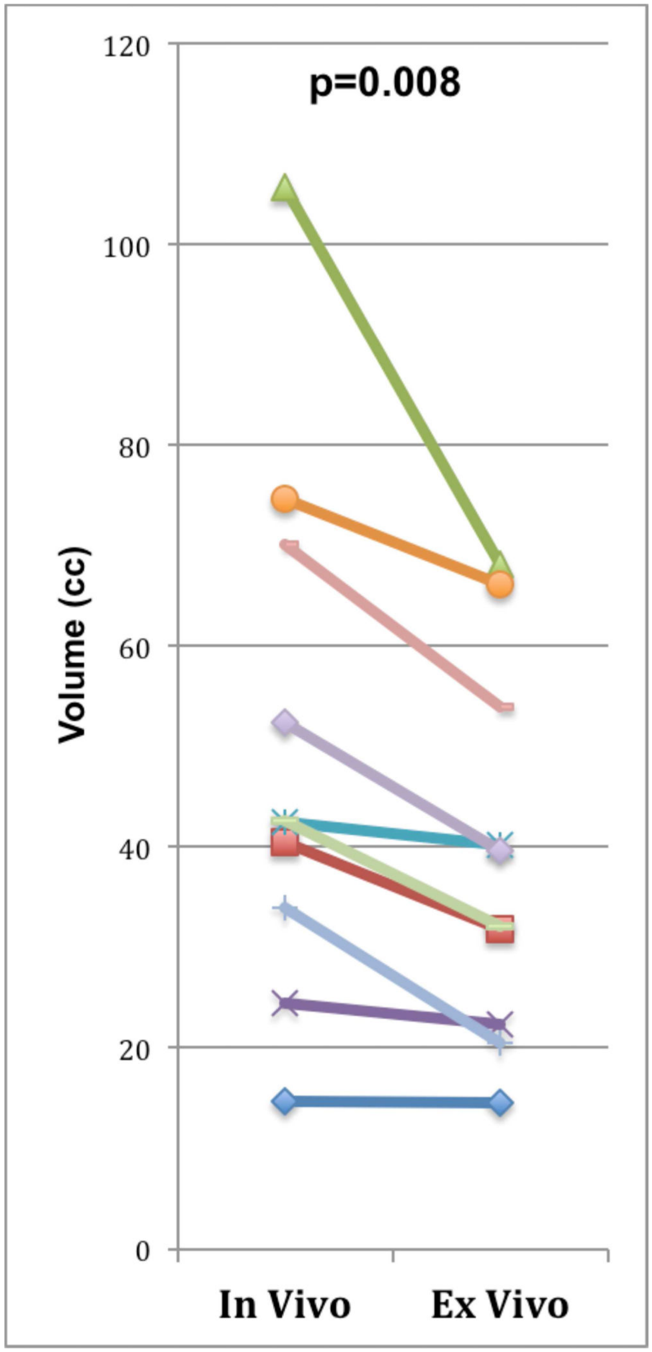

Figure 1.

Comparison of *in-vivo* and *ex-vivo* prostate volumes in 10 patients. *p*-Value represents result of paired *t*-test comparing the two sets of data.

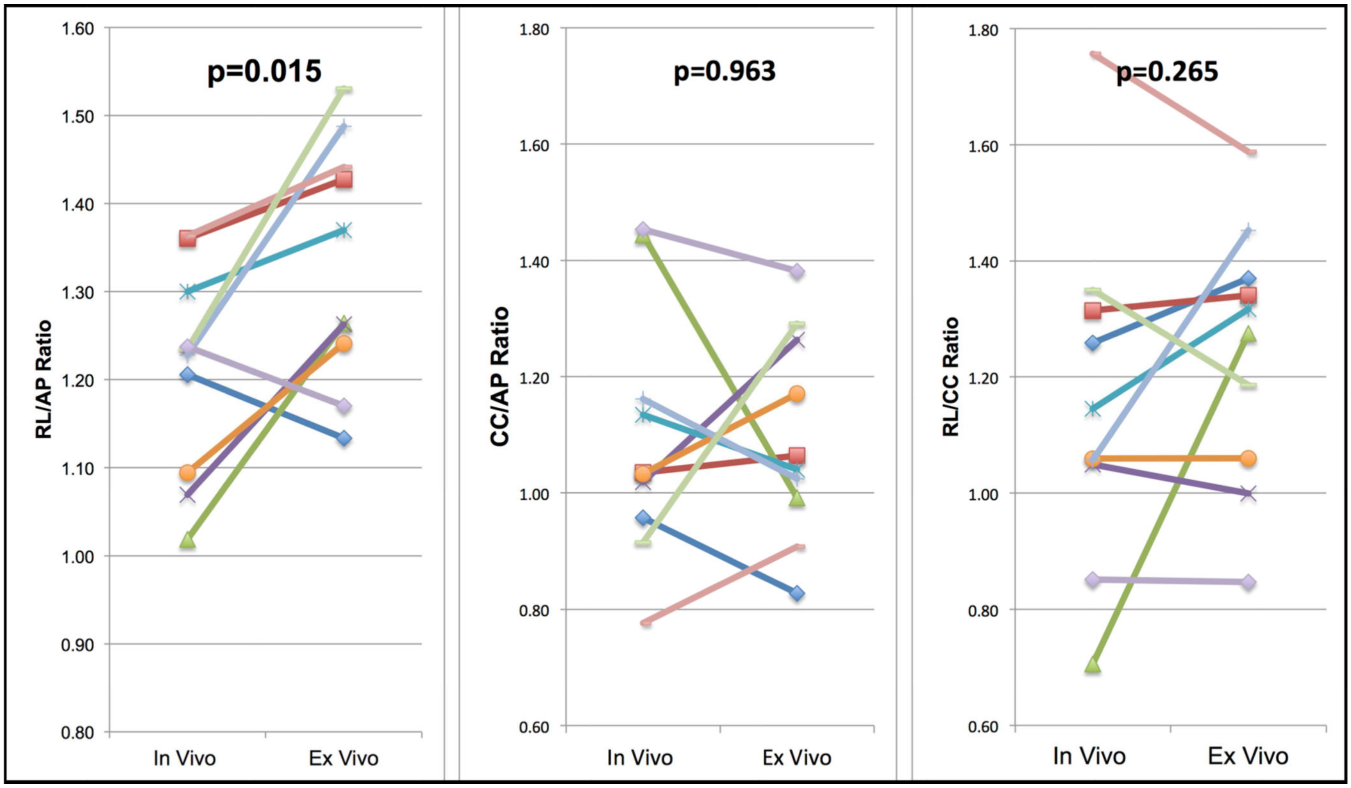

Figure 2.

Comparison of *in-vivo* and *ex-vivo* ratios of linear prostate dimensions in 10 patients. *p*-Value represents result of paired *t*-test comparing the two sets of data.

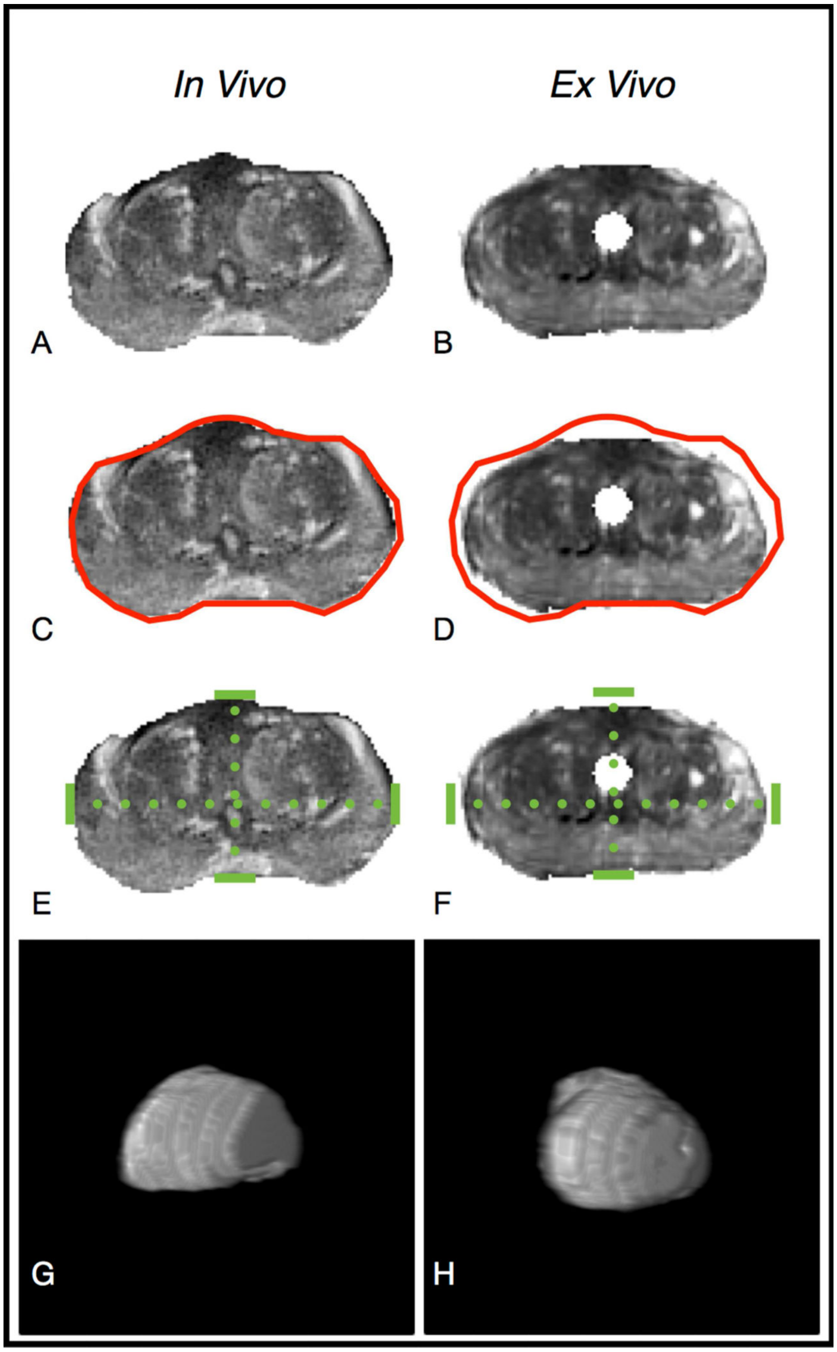

Figure 3.

Change in volume and shape between *in-vivo* and *ex-vivo* MRI. Axial T2WI images at the level of the verumontanum are shown for (a) *in-vivo* and (b) *ex-vivo* acquisitions for a single patient. (c–d) Images depict an identical red contour reflecting the external contour of the (c) *in-vivo* prostate, although superimposed on the prostate in both images and demonstrating the smaller size of the (d) *ex-vivo* prostate. (e–f) Images depict identical dotted green lines reflecting the RL and AP dimensions of the (e) *in-vivo* prostate, although superimposed on the prostate in both images and demonstrating the change in relation between these lines in the (f) *ex-vivo* prostate. (g–h) Images depict a three-dimensional, rendered, shaded surface display of the (g) *in-vivo* and (h) *ex-vivo* prostate, generated from the two sets of T2WI images, demonstrating a difference in prostate shape between the two scans; the prostate exhibits its typical pyramidal shape in the *in-vivo* scan and a relatively spherical shape in the *ex-vivo* scan.

Table 1

Comparison of volume and shape assessments between *in vivo* and *ex vivo* MRI

	***In-vivo* MRI**	***Ex-vivo* MRI**
Volume		
Mean±SD (cc)	50.8±26.8	39.7±18.6
p-Value[a]	0.008	
Average percent change[b]	−19.5	
Median percent change[b]	−22.3%	
RL/AP ratio		
Mean±SD	1.21±0.12	1.33±0.14
p-Value[a]	0.015	
Average percent change[b]	12.2%	
Median percent change[b]	11.3%	
CC/AP ratio		
Mean±SD	1.09±0.22	1.10±0.18
p-Value[a]	0.963	
Average percent change[b]	0.34%	
Median percent change[b]	−2.1%	
RL/CC ratio		
Mean±SD	1.15±0.29	1.24±0.22
p-Value[a]	0.265	
Average percent change[b]	8.8%	
Median percent change[b]	1.3%	

[a] Listed in bold when statistically significant at $p<0.05$.

[b] Change from *in-vivo* to *ex-vivo* measurements.

RL/AP ratio, right-to-left/anteroposterior ratio; CC/AP ratio, craniocaudal/anteroposterior ratio; RL/CC ratio, right-to-left/craniocaudal ratio.